REPRINTED FROM:

ADVANCES IN FIBER COMPOSITE MATERIALS

Edited by

TAKEHITO FUKUDA

Osaka City University, Japan

ZENICHIRO MAEKAWA

Kyoto Institute of Technology, Japan

TORU FUJII

Doshisha University, Japan

Current Japanese Materials Research—Vol. 12

ELSEVIER

AMSTERDAM · LONDON · NEW YORK · TOKYO 1994

Advances in Fiber Composite Materials
Edited by T. Fukuda, Z. Maekawa and T. Fujii

CHAPTER 3

Fracture Mechanism for High-Modulus Pitch-Based CFRP

EIKI TSUSHIMA,[1] JUN TAKAYASU,[1] and ISAO KIMPARA[2]

[1]*Corporate Research and Development Laboratory, TONEN Corporation, 1-3-1 Nishi-tsurugaoka, Ohi-machi, Iruma-gun, Saitama 356, Japan*
[2]*Dept. of Naval Architecture and Ocean Engineering, The University of Tokyo, 7-3-1 Hongo, Bunkyo-ku, Tokyo 113, Japan*

ABSTRACT

The fracture mechanism for high-modulus pitch-based carbon fiber reinforced plastic (CFRP) was experimentally investigated by preparing CFRP from fibers with various surface treatment levels and with two kinds of matrix resin. The results show that the CFRP strength was significantly affected by the fiber surface treatment level. This was particularly marked for CFRP with the hard matrix resin used in this study.

The inter-laminar shear strength (ILSS) increased with increasing level of surface treatment. On the contrary, the longitudinal tensile strength (σ_t) decreased. Both strength figures were constant for a range of surface treatment level exceeding the standard level.

The reason for these results was clarified by observations on a test with a single embedded fiber, this experiment being a popular method to determine the interfacial strength between a fiber and matrix resin. The results show that there were two different modes of adhesive failure at a critical fiber length, one due to fiber debonding, and the other to matrix yielding. These test results enable the effect of surface treatment on CFRP mechanical properties to be predicted.

Keywords: CFRP, fracture mechanism, surface treatment, pitch-based carbon fiber, ILSS

INTRODUCTION

Pitch-based carbon fiber has recently been developed by several Japanese companies. A remarkable feature of pitch-based carbon fiber is its high modulus, which can reach over 700 GPa. More recently, the tensile strength

has been improved so that pitch-based carbon fiber has potential applications not only in advanced technology fields such as aerospace, but also in general mechanical structures.

However, the mechanical properties of pitch-based CFRP have not been sufficiently clarified. There are so many factors affecting the properties of CFRP that it is difficult to obtain a meaningful estimate of the strength.

Accordingly, this present work experimentally examines the tensile fracture mechanism for high-modulus pitch-based carbon fiber reinforced plastics.

EXPERIMENTAL PROCEDURE

Carbon fiber

FORCA FT700 and FT500 high-modulus pitch-based carbon fiber, manufactured by TONEN Corporation, and two different types of matrix resin were used in this study. Typical properties are given in Tables 1 [1] and 2. The fiber surface is treated to improve the transverse strength of CFRP laminates, and treatment by electrochemical oxidation generally produces active functional groups on the surface [2]. Several surface-treated fibers were used in this study, with treatment levels selected from

TABLE 1
Typical properties of FORCA carbon fiber

Fiber name		*FT700*	*FT500*
Filament diameter	(μm)	10	10
Density	(10^3 kgm^{-3})	2.16	2.14
Tensile strength	(GPa)	3.8	3.5
modulus	(GPa)	700	500
failure strain	(%)	0.54	0.70
Coefficient of thermal expansion	(1/K, 10^{-6})	−1.5	−1.0
Thermal conductivity	(W/M/K)	360	150
Specific heat	(cal/g°C)	0.17	0.17
Electrical resistivity	(Ω cm, 10^{-4})	5	8

TABLE 2
Typical resin properties

Resin name		*Ep-828*[a]	*Ep-828*[a]
Hardener		HN-5500[b]	DDS[c]
Curing temperature	(°F)	250	350
time	(hr)	2	2
Tensile strength	(MPa)	78	67
modulus	(GPa)	3.0	3.5
failure strain	(%)	7.6	3.1
Glass transition temp.	(°F)	320	428
Izod impact strength	(kg cm/cm^2)	2.5	1.1

[a] Manufactured by Yuka Shell Co. Ltd. Japan.
[b] Manufactured by Hitachi Chemical Co. Ltd. Japan.
[c] Diamino diphenyl Sulphone.

1/5 to 100 times the standard surface treatment level. Apart from the surface chemical properties, the fiber mechanical properties were not changed by performing this surface treatment. This has been confirmed by a fiber tensile test.

Measurement of the interfacial strength

Two main approaches were taken to determine the interfacial strength between the fiber and matrix resin, one involving tests with a single fiber, and the other with unidirectional laminates in accordance with ASTM D-2344 (inter-laminar shear strength (ILSS) test). ILSS test specimens were made with the Ep-828/HN5500 resin, which was the same matrix as that used with the single-strand specimen for the tensile test.

Figure 1 illustrates a single-fiber test specimen embedded to observe the breaking behavior in an epoxy resin (Ep-828/S-Cure661, Nihon Kayaku Co. LTD. Japan) and to measure the interfacial shear strength [3, 4]. The Ep-828/S-Cure661 matrix resin had almost the same mechanical properties as those of the Ep-828/HN5500 resin, and the specimen consisted of a single fiber embedded in the surface of the resin. This was subjected to a tensile strain greater than the ultimate fiber strain. The fiber

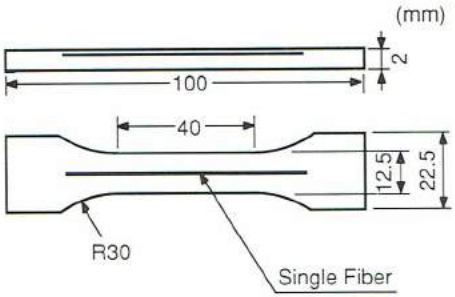

FIG. 1. Dimensions of the embedded single-fiber specimen.

eventually broke into small segments within the matrix. Assuming that the fiber strength was uniform along the length of the fiber, the interfacial shear strength can be calculated from the fiber tensile strength, fiber diameter, and fiber segment length, as follows [5]:

$$(l_c)_{ten} = \tfrac{4}{3}(\bar{l})_{ten}, \tag{1}$$

where $(\bar{l})_{ten}$ is the mean fragment length, and

$$(l_c)_{ten} = \frac{(\sigma_f) \times d}{2 \times \tau}, \tag{2}$$

$$\sigma_f = \sigma \times (25/l_c)^{(-1/m)}, \tag{3}$$

where τ is the yielding shear strength at the fiber–matrix interface; d is the diameter of the fiber; σ_f is the fiber tensile strength of a segment; σ is the fiber tensile strength of a 25 mm length; and m is the Weibull statistical shape parameter ($m = 8.0$ for FT500).

Measurement of the tensile strength

Unidirectional (UD) CFRP strand specimens were prepared by using the conventional method (ASTM D-4018, JIS R-7601). Carbon fiber tow was impregnated with epoxy resin and cured at 250°F for Ep-828/HN5500, and at 350°F for Ep-604/DDS resins. The fiber volume fraction of a specimen was about 50%, but the total fiber cross-sectional area was accurately determined from the density of the fiber and texture as follows:

$$A = (\text{Tex})/(\text{Den}) \times 10^{-3}, \tag{4}$$

where A is the total cross-sectional area of a fiber strand specimen (mm^2);

Tex is the texture of carbon fiber tow (kg/km); and Den is the carbon fiber density (g/cm^{-3}).

EXPERIMENTAL RESULTS

ILSS test results

Figure 2 shows the ILSS test results as a function of the surface treatment. These are similar to the results for PAN-based carbon fiber reinforced plastic [6]. The horizontal axis is a measure of the fiber surface treatment level; the standard surface treatment is shown as level 1. This relationship can be divided into two zones in the figure, an increasing zone and a constant zone for ILSS. It is easy to understand that ILSS would increase with increasing level of surface treatment, but the question arises as to why ILSS takes on a constant value when the treatment is a little above the standard level. This phenomenon can be explained by the interfacial strength exceeding the matrix resin yielding shear strength, which is the point above which permanent deformation takes place. The embedded single-fiber test results explain this phenomenon more clearly.

Embedded single-fiber test results

Four differently surface-treated fiber samples were evaluated by the embedded single-fiber test, the results being given in Fig. 3. The interfacial

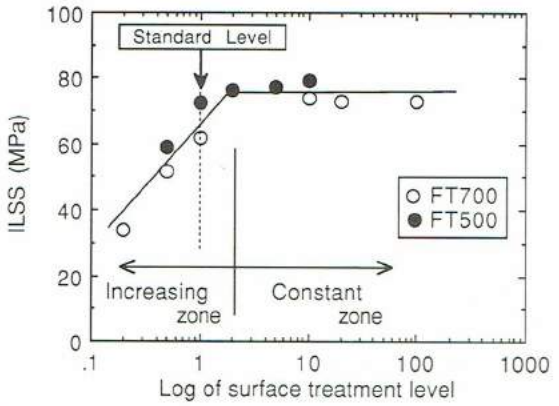

FIG. 2. Relationship between ILSS and surface treatment. (Matrix resin: Ep-828/HN5500).

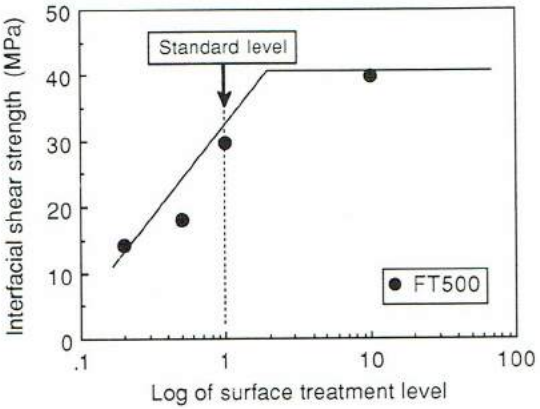

FIG. 3. Embedded single-fiber test results for the interfacial shear strength between FT500 and Ep-828/S-Cure661.

shear strength (τ) obtained by the single-fiber test initially increased with increasing surface treatment level. These experimental results could also be approximated by two straight lines, similarly to the ILSS test results (Fig. 2). Figure 4 shows the relationship between ILSS and τ; there is a good correlation between the two factors.

Using a polarizing microscope, Fig. 6 shows the photoelastic stress patterns in the epoxy matrix near the ends of a broken fiber segment for

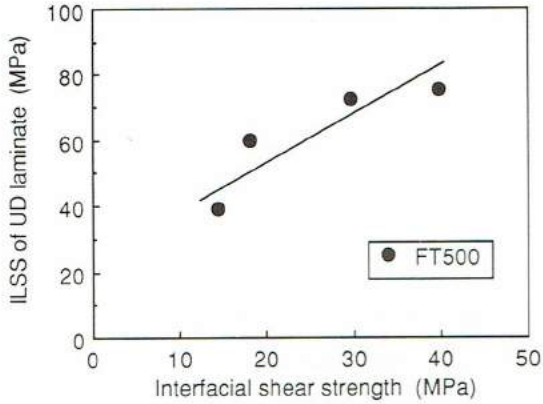

FIG. 4. Relationship between ILSS and interfacial shear strength.

surface treatment levels of 1/5 and 10 times the standard level for FT500 fiber. A cyclic strain was applied to each specimen, the level of which is given in Fig. 5, and observations were made while the specimen was under load and again after the load had been released. Fiber breakage occurred at a strain of about 1.0% in the two specimens, but as the strain was increased, a difference related to the interfacial strength was observed. The number of fiber breakage points was greater for the 10× treatment level than for the 1/5× level, the critical fiber length being 0.6 mm for the 10× fiber and 1.2 mm for the 1/5× fiber. According to the observations, under load, of the 10× treatment level fiber, as the sample strain increases, an elliptically shaped region, indicating a high shear-stress zone, moves further away from the fiber breakage points and leaves a narrow highly stressed region which looks like the beak of a bird. It is considered that this narrow, highly stressed region shows that the yielding zone of the matrix resin is caused by shear stress. Thus, the narrow, highly stressed region remains after the load has been released (pictures C′, D′ and E′ of the 10× treatment level fiber). On the other hand, a different photoelastic stress pattern can be seen in the 1/5× treatment level fiber. With increasing strain, a bright region spread along the fiber, and high magnification showed that fiber–matrix debonding was occurring.

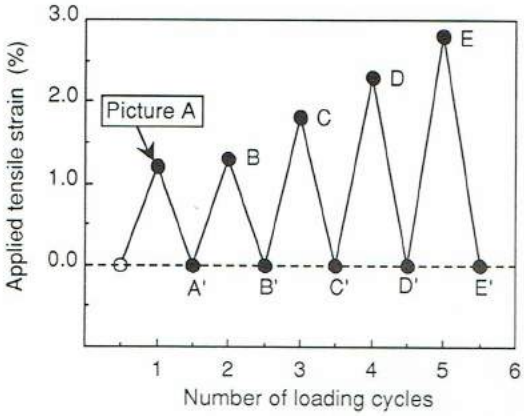

FIG. 5. Cyclic loading pattern for the embedded single-fiber test (● are observed points). Note: Strain was measured in the test specimen, and not in the embedded fiber.

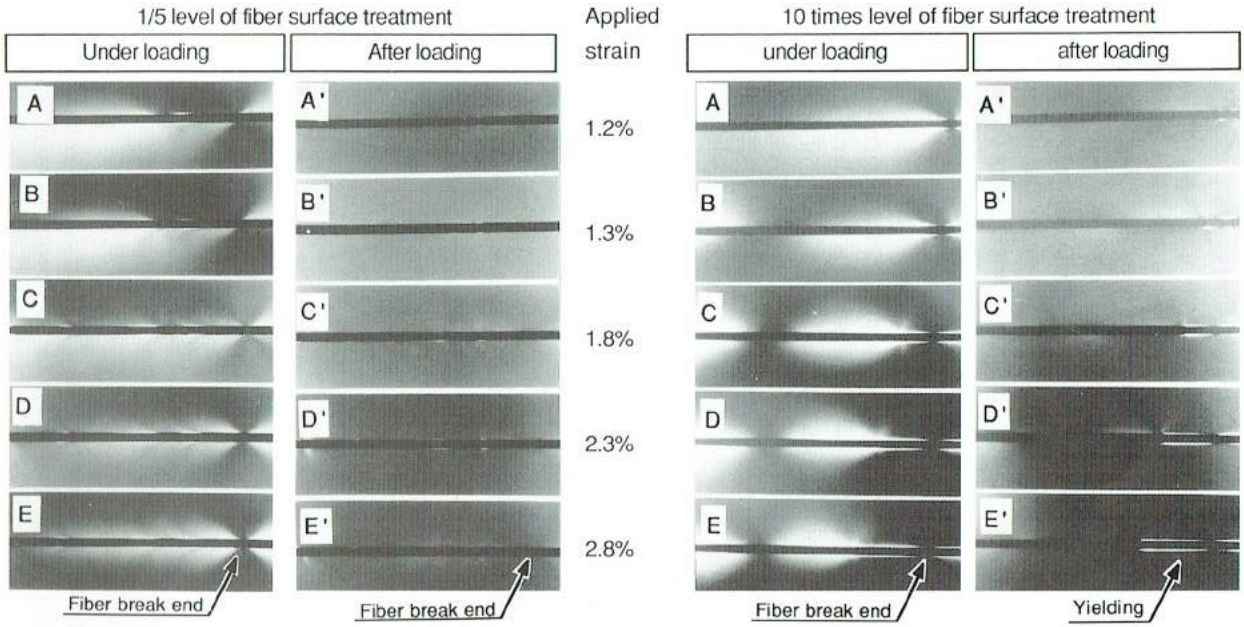

FIG. 6. Polarized microphotographs of FT500 in an embedded single-fiber test.

The test results, just described, mean that the interfacial strength between the fiber and matrix resin exceeded the matrix yielding shear strength. Thus, in the case of surface treatment below the standard level, the mechanical properties of CFRP change with surface treatment, and in the case above the standard level of treatment, the properties are determined by the matrix resin. This interpretation is also confirmed by the tensile test results.

Tensile strength test results

Two different resin systems were used for the test, one being a 250°F curing resin, Ep-828/HN5500, and the other a 350°F curing type, Ep-604/DDs, which is a more brittle and harder matrix. Figure 7 shows the longitudinal tensile test results of CFRP samples as a function of the surface treatment level. The tensile strength decreases with increasing surface treatment level up to the standard treatment level (fiber debonding level). In the range from 10× to 100× surface treatment level (matrix yielding level), the strength remains constant, although the figure for the Ep-828 resin CFRP is higher than that for the Ep-604 material in the zone of matrix yielding. It can be assumed that CFRP follows the fiber-breakage propagation model [7]. This model infers that, as each fiber breaks, the redistribution of stress leads to additional stress on neighboring fibers, i.e., there is a stress magnification effect. Thus, there is increased probability that fracture will occur in the immediately adjacent fibers. In this model, stress redistribution is subject to the interfacial strength or matrix yielding

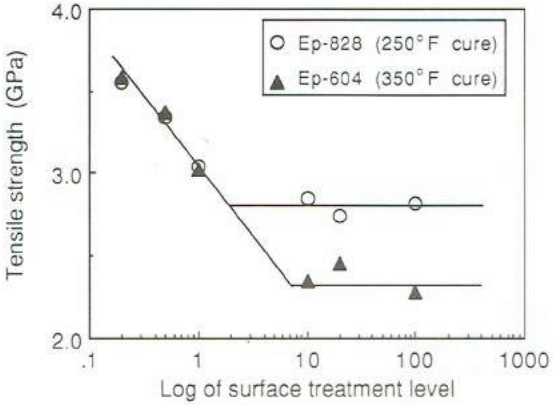

FIG. 7. Tensile strength of a FT700 single strand with two different matrix resins.

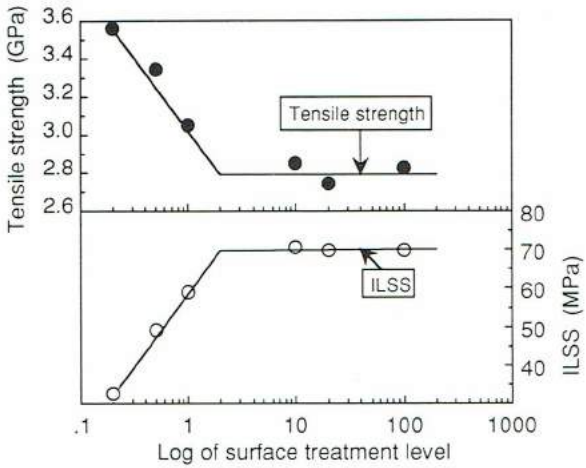

FIG. 8. ILSS and tensile strength of FT700/Ep-828.

strength. Thus, the strength of the Ep-604 CFRP was significantly less in the range of surface treatment level from 10× to 100×, because the strength was controlled by matrix yielding. Ep-604 is harder than Ep-828 resin. In the case of the lower-than-normal surface treatment level, the strength was equal with the two matrix resin systems, because stress redistribution is not controlled by the matrix but by the interfacial strength, which corresponds to the surface treatment level.

Figure 8 shows the ILSS and the tensile strength as functions of surface treatment level on one graph. There is a very good correlation between the two factors, which is clearly explained by the single-fiber test results.

Effect of temperature

From the test results just described, tensile strength was affected by the matrix yielding shear strength at excessive surface treatment levels. Thus, CFRP tensile strength dropped significantly. However, if the test temperature is high enough for the resin to remain soft, the tensile strength can be expected to be higher than the strength at normal temperature. To confirm this prediction, tests on FT700/Ep-604 at 350°F were conducted. The result indicates that the tensile strength rose to 3.0 GPa from 2.3 GPa under elevated temperature conditions.

DISCUSSION

FEM simulation

The mechanical properties of CFRP were experimentally investigated by using several differently surface-treated fibers and with different matrix resins. However, because it took so much effort to obtain useful test results, a more effective method for failure simulation is desirable. Many researchers have attacked this problem in various ways, and many simulation methods have been suggested. We will discuss a trial of the most suitable simulation method for the tensile failure process in UD CFRP [8, 9]. CFRP with two different interfacial strength fibers of 7.2 μm diameter, 400 GPa tensile modulus, and 3500 MPa tensile strength will be considered.

Analytical model

The model consists of isoparametric finite elements which are connected by normal and shear spring elements between adjacent nodes. The mechanical properties of the fiber, matrix, and interfaces are given by the spring elasticity and strength, while the strength of a fiber element is based on a Weibull distribution. If the fiber diameter is assumed to be 7.2 μm, its width is 6.4 μm in a two-dimensional model. Figure 9 shows a schematic diagram of the interfacial spring elements in this FEM simulation model.

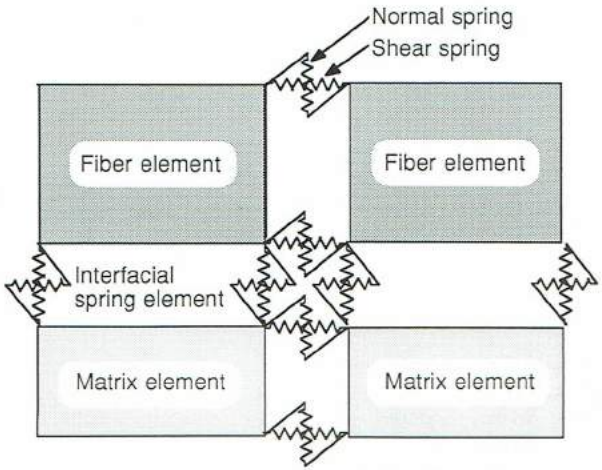

FIG. 9. Schematic diagram of the interfacial spring elements.

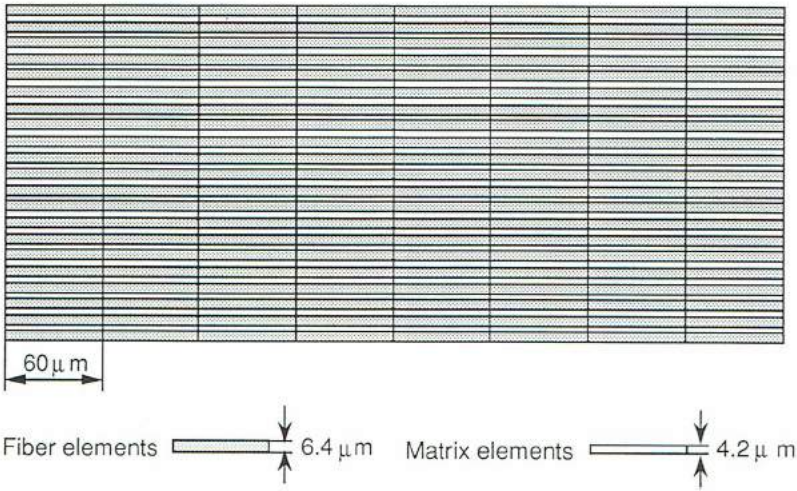

FIG. 10. FEM simulation model for unidirectional CFRP.

The elements are connected by normal and shear spring elements between two adjacent nodes. Figure 10 shows a micro-model of CFRP consisting of 21 × 8 fiber elements and 20 × 8 matrix elements. The length of each element is assumed to be equal to the ineffective length, which can be determined by the embedded single-fiber test. The material constants of the fiber and matrix are given in Table 3, while the interfacial strength is assumed to be 50 MPa for low-strength interfacial fiber and 100 MPa for

TABLE 3
Material properties for the FEM simulation

				Interfacial strength	
		Fiber	*Matrix*	*Low-strength fiber*	*High-strength fiber*
Tensile modulus	(GPa)	400	3.5	3.5	3.5
Shear modulus	(GPa)	154	1.25	1.25	1.25
Tensile strength	(MPa)	3500	120	50	100
Shear strength	(MPa)		100	50	100
Weibull shape parameter		6.98			

high-strength interfacial fiber. These can be roughly estimated from the ILSS test results.

Simulation method

A dynamic FEM simulation was performed on a unidirectional CFRP lamina model based on the Newmark β method. The dynamic failure process was simulated as time proceeded by breaking the spring elements one by one after applying the maximum stress criterion. A load increment scheme was applied, in which the load was increased until a succeeding failure started if no failure had taken place in spring elements during three successive time intervals. The interval was set at $\Delta t = 0.02\,\mu s$.

Simulation results

The dynamic simulation was undertaken 20 times, changing the strength distribution of the fiber randomly for each condition of interfacial shear strength. The results of this FEM simulation are listed in Table 4, indicating that the mean tensile strength was larger and the variation in tensile strength smaller with the lower level surface treated fiber composite. This agrees very well with the experimental results. Typical examples of the simulated failure patterns for models are shown in Fig. 11, where the thick lines indicate interfacial failure between the fiber and matrix. Typical tensile failure surfaces of UD CFRP are shown in Fig. 12. We conclude that the FEM simulated failure pattern agrees with the actual fractured surface from SEM observations.

This FEM simulation deals with the micro-model of a composite, but an actual composite consists of many micro-models. The fracture of one micro-model would not always cause the fracture of the whole composite. Thus, there are some problems in applying the micro-model simulation to actual composite fractures. However, the authors have already published an idea that clarifies the relationship between the micro-model and the macro-model, the latter applying to an actual composite [10].

TABLE 4
The results of the FEM simulation

Interfacial strength	*Failure stress*	*C.V. (%)*	*Failure strain*
50 MPa fiber	1.41 GPa	7.3	0.625%
100 MPa fiber	1.18 GPa	12.4	0.489%

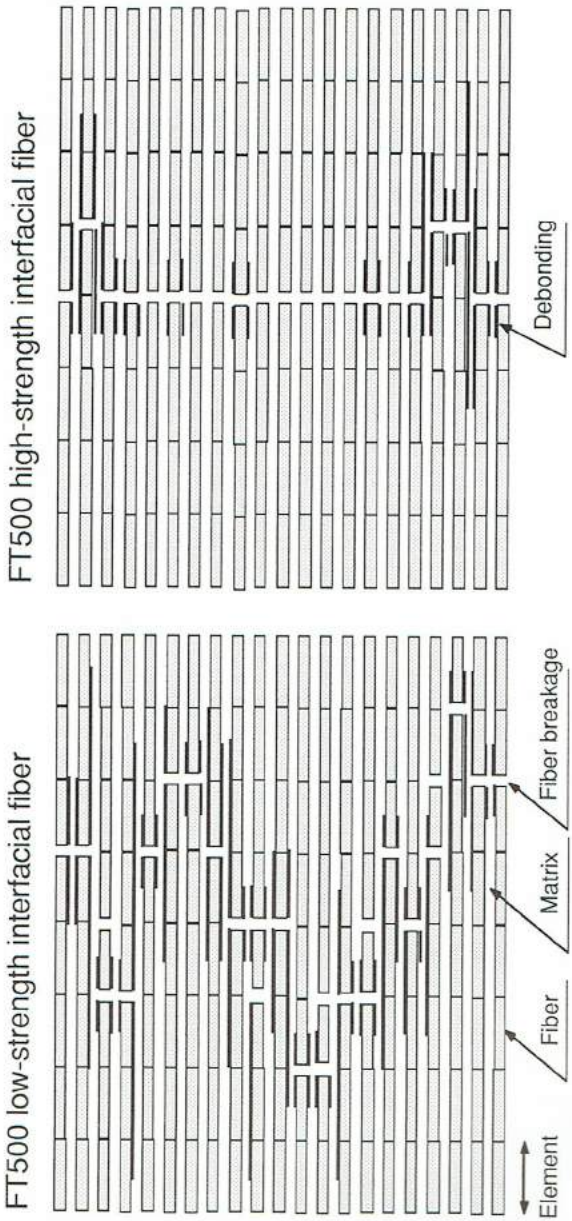

FIG. 11. Typical simulated failure patterns in unidirectional CFRP models.

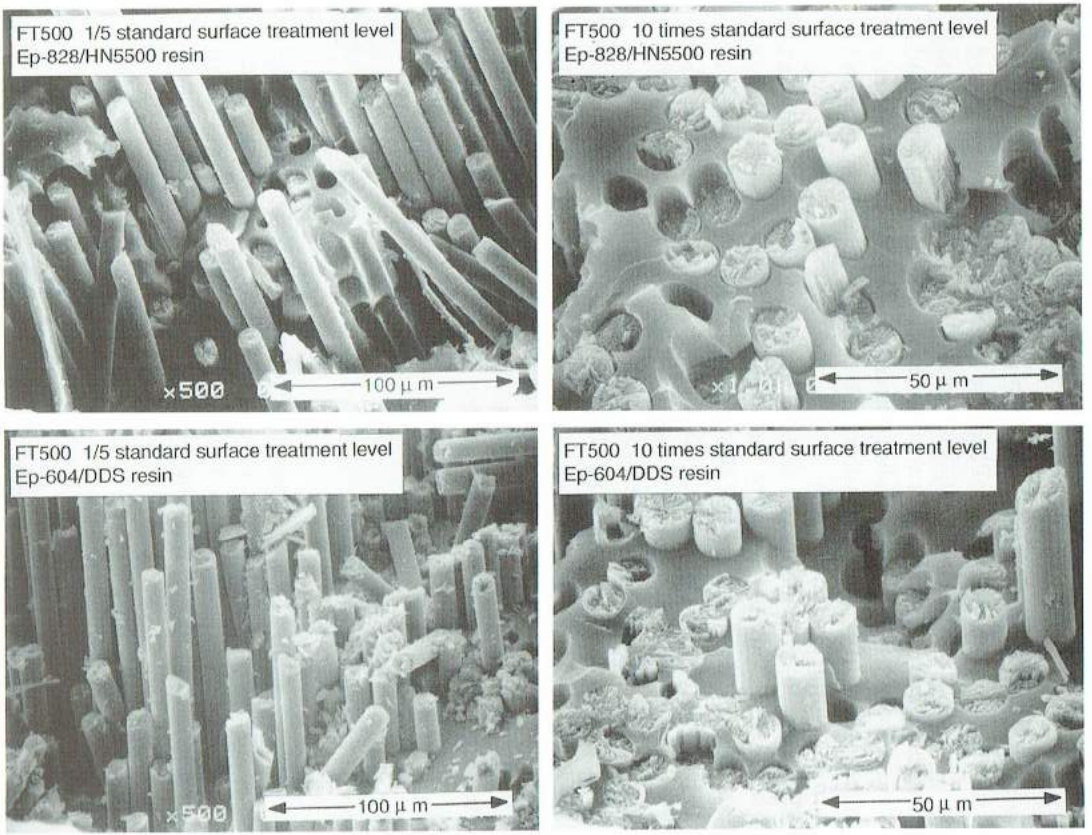

FIG. 12. SEM observations of tensile-fracture surfaces (FT500 single strand specimens with different surface treatment).

CONCLUSIONS

The mechanical properties of UD CFRP were investigated. The interfacial shear strength between a fiber and the matrix resin was determined by the embedded single-fiber test. The results show that the strength increased with increasing surface treatment level up to certain points, and could exceed the matrix yielding shear strength. The adhesion between a fiber and the matrix could be classified into the fiber debonding type and the matrix yielding type.

ILSS increased with increasing surface treatment up to the standard level, which represents adhesion of the fiber debonding type. ILSS was constant for adhesion in the matrix yielding range. On the other hand, UD CFRP tensile strength decreased with surface treatment level, and the strength was constant for adhesion in the matrix yielding range. The tensile strength was determined by the surface treatment level in the range for fiber debonding, while the matrix yielding shear strength controlled the tensile strength above the standard surface treatment level. The tensile strength decreased markedly for CFRP with excessively surface-treated fiber when a hard matrix resin was used. The fracture mechanism for high-modulus pitch-based CFRP could be explained by the fiber-break propagation model.

ACKNOWLEDGEMENTS

The authors thank Dr. T. Ohsawa, Professor, and Dr. M. Miwa, Associate Professor, both of Gifu University, for their consultation on the embedded single-fiber tests. We also thank Mr. K. Inoue of TONEN Corp. for his FEM calculations in this study.

REFERENCES

[1] E. Tsushima, *Proc. of 34th Intern. SAMPE Symp. and Exhib.*, 2042 (1989).
[2] E. Fitzer, H. Jager, N. Ropovska and F.V. Sturm, *J. Appl. Electrochem.*, **18**, 178 (1988).
[3] A. Kelly and W.R. Tyson, *J. Mech. Phys.*, **14**, 177 (1966).
[4] L.T. Drzal, M.J. Rich and P.F. Lloyd, *J. Adhesion*, **16**, 1 (1982).
[5] T. Ohsawa, A. Nakayama, M. Miwa and A. Hasegawa, *J. Appl. Polym. Sci.*, **22**, 3203 (1978).

[6] T. Norita, J. Matsui and H.S. Matsuda, *Proc. of 1st Intern. Conf. on Composite Interface (ICCI-I)*, 123 (1986).
[7] D. Hull, *An Introduction to Composite Materials*, Cambridge University Press, 135 (1981).
[8] I. Kimpara, E. Tsushima and H. Yoshizawa, *Proc. of 7th ICCM Conf.*, 73 (1989).
[9] I. Kimpara, K. Kageyama, E. Tsushima, J. Takayasu and K. Inoue, *Proc. Japan-U.S. CCM-V*, 521 (1990).
[10] I. Kimpara, T. Ozaki and K. Inoue, *Bull. Soc. Naval Architects of Japan*, **163**, 423 (1988).